# Assessment of hail damages in maize using remote sensing and comparison with an insurance assessment: A case study in Lombardy

**Calogero Schillaci,[1,2] Fabio Inverardi,[2] Martin Leonardo Battaglia,[3] Alessia Perego,[2] Wade Thomason,[3] Marco Acutis[2]**

*[1]European Commission, Joint Research Centre, Ispra (VA), Italy; [2]Department of Agricultural and Environmental Sciences Production, Landscape, Agroenergy, University of Milan, Milan, Italy; [3]Centre for Sustainability Science, The Nature Conservancy, Arlington, VA, USA*

## Highlights

- *The discovery rate of damaged fields improved.*
- *MSAVI outperformed NDVI and other vegetation indices, identifying 73.3% of occurrences.*
- *Estimation of damage from remote sensing was more accurate for fields severely affected >50%.*
- *In low-intensity hail events (<50 canopies affected), the MSAVI provided a detailed picture of the damage across the field.*
- *The proposed approach is promising to develop a 'sampling map' for detailed on-ground assessment.*

Correspondence: Calogero Schillaci, European Commission, Joint Research Centre, via E. Fermi 2749, 21027 Ispra (VA), Italy.
E-mail: calogero.schillaci@ec.europa.eu

Key words: Hailstorms; damage estimation; vegetation indices; modified soil-adjusted vegetation index; change detection.

Acknowledgements: the authors are grateful to Annunzio D. and Albertini G., who provided the field surveys insurance assessments in 2018; ESA Sentinel mission; Landsupport H2020 project ID 774234; reviewers who improved the early draft of the manuscript.

Contributions: CS, FI, MA, conceptualisation, software, resources, data curation, original draft preparation; FI, CS, MB, AP, MA, methodology; FI, validation; CS, FI, MB, AP, WT, MA, review and editing; FI, CS, visualisation; MA, supervision, funding acquisition. All authors have read and agreed to the published version of the manuscript.

Conflict of interest: the authors declare no potential conflict of interest.

Received for publication: 24 June 2022.
Revision received: 12 September 2022.
Accepted for publication: 4 October 2022.


*Licensee PAGEPress, Italy*
*Italian Journal of Agronomy 2022; 17:2126*
*doi:10.4081/ija.2022.2126*



## Abstract

Studies have shown that the quantification of hail damage is generally inaccurate and is influenced by the experience of the field surveyors/technicians. To overcome this problem, the vegetation indices retrieved by remote sensing, can be used to get information about the hail damage. The aim of this work is the detection of medium-low damages (*i.e.*, between 10 and 30% of the gross saleable production) using the much-used normalized difference vegetation index (NDVI) in comparison with alternative vegetation indices (*i.e.*, ARVI, MCARI, SAVI, MSAVI, MSAVI2) and their change from pre-event to post-event in five hailstorms in Lombardy in 2018. Seventy-four overlapping scenes (10% cloud cover) were collected from the Sentinel-2 in the spring-summer period of 2018 in the Brescia district (Lombardy). An unsupervised classification was carried out to automatically identify the maize fields (grain and silage), testing the change detection approach by searching for damage by hail and strong wind in the Lombardy plain of Brescia. A database of 125 field surveys (average size 4 Ha) after the hailstorm collected from the insurance service allowed for the selection of the dates on which the event occurred and provided a proxy of the extent of the damage (in % of the decrease of the yield). Hail and strong wind damages ranged from 5 to 70%, and they were used for comparison with the satellite image change detection. The differences in the vegetation indices obtained by Sentinel 2 before and after the hailstorm and the insurance assessments of damage after the events were compared to assess the degree of concordance. The modified soil-adjusted vegetation index outperformed other vegetation indices in detecting hail-related damages with the highest accuracy (73.3%). On the other hand, the NDVI resulted in scarce performance ranking last of the six indices, with an accuracy of 65.3%. Future research will evaluate how much uncertainty can be found in the method's limitations with vegetation indices derived from satellites, how much is due to errors in estimating damage to the ground, and how much is due to other causes.

## Introduction

### Maize cultivation in Italy

With an average total production of around 6.5 million Mg (range: 6.05-7.07) harvested in an area of 1,030,000 ha (650,000 ha grain; 380,000 maize silage) during the period 2015-2019 (FAOSTAT, 2021; ISTAT, 2021), Italy is one of the leading maize producers in Europe (EUROSTAT 2021). Around 90% of this total maize production is concentrated in the Po Valley (Berti *et al*., 2019). However, in Italy, maize cultivation has declined over the last 15 years, primarily due to the relatively low maize grain prices and high production costs (USDA, 2017). In 2006, the Italian national institute of Statistics (ISTAT, 2006) estimated a 1,383,000 ha of maize-growing area, of which 1,108,000 ha corresponded to grain maize and 275,000 ha to silage maize. Despite this recent decline, Maize harvested for grain still represents a critical component of Italian agriculture, with a total estimated economic value of 1074, 1043, and 1126 million EUR in 2018, 2019, and 2020, respectively, placing Maize as the second most valuable crop in the country, only after wheat production (European Commission, 2021).

The impacts of hail events on crops have received little attention from the agronomy community. Among abiotic stresses, damage by hail is one of the most prevailing and destructive (Changnon *et al*., 2009; Klein and Shapiro, 2011; Punge and Kunz, 2016; Battaglia *et al*., 2019a, 2019b). Hail, defined as a set of irregular ice bodies that form in convective clouds (Kunkel and Changnon, 2003), causes significant damage to crops (Prabhakar *et al*., 2019). In regions where the occurrence of hailstorms is common, such as in mid-latitudes across the world, it can have a significant impact on the growth of crops, and it is predicted that increasing climate change may increase the frequency of these extreme weather events (Piani *et al*., 2005; Diffenbaugh *et al*., 2013), and the associated losses in agricultural production (Torriani *et al*., 2007). On a global scale, hail events have reportedly risen in the last decades (Vescovo *et al*., 2016). Contrarily, data collected in the U.S. suggests that hailstorms and consequential damage to crops and properties decreased from 1950 to 2009 (Botzen *et al*., 2010). In Europe, potential damages due to hailstorms with a return period of 200-300 years were estimated to be around 4 billion EUR (Zimmerli, 2005), and reports suggest that severe thunderstorms and extreme events associated with harmful atmospheric agents in the continent are on the rise (Mohr and Kunz, 2013). In Italy, the hailstorms are mainly concentrated in the northern part of the country: the Po Valley and the Pre-Alps, specifically in Lombardy and Veneto (Baldi *et al*., 2014; Punge *et al*., 2014). Maize farming is prevalent in this region, accounting for 90% of Italian maize production (ISTAT, 2021). Typically, the maize sowing period in Italy ranges from the end of March until mid-May, with the most considerable growth rates occurring in June, July, and August, when the risk of hailstorms in the country is maximum. In the US, the National Weather Service defines severe hail when they reach 25.4 mm in diameter. Farmers and the agricultural community consider hail severity according to the impacts on crops. Small hail in large volumes or driven by strong winds is the worst scenario for farmers since hail can strip crop heads and stalks (Childs *et al*., 2020). The mechanical impact of hail on the maize canopy and the consequent damage to plants has been well documented over the last 50 years (Hanway, 1969; Hicks *et al*., 1977; Shapiro *et al*., 1986; Klein and Shapiro, 2011; Battaglia *et al*., 2018; Thomason and Battaglia, 2020). Hail reduces grain yield by shredding leaf blades and reducing the photosynthetic area (Dungan, 1934; Jenkins, 1941; Hanway, 1969; Vorst, 1993; Klein and Shapiro, 2011). When hailstorms occur at the early growing stages of maize, plants are typically broken at the soil surface level, reducing plant stands (Dungan, 1934; Vorst, 1993; Nielsen, 2012). In maize plants, hail damage can interfere with the movement of assimilates in the plant (Dungan, 1934). Moreover, damage by hail can trigger pathogens attacks and leaves losses, further reducing the loss of photosynthetically active areas and, with this, the reduction in grain yield (Johnson, 1978; Grotjahn, 2021) and the amount of biomass collected (Furlanetto *et al*., 2021).

The timing (*i.e*., the phenological stage when hail damage occurs) and the severity of defoliation (percentage of leaf damaged or removed) are the main variables determining the degree of damage in maize plants subjected to hail events (Hanway, 1969; Battaglia *et al*., 2018, 2019b). Complete defoliations up to the V6-V7 according to the BBCH scale (Meier *et al*., 2009), growth stages (collar method; Abendroth *et al*., 2011) usually cause minimal to no reduction in the final grain yield, as the plant growing point is still below the soil surface until this time (Vorst, 1993; Lee, 2007; Klein and Shapiro, 2011; Battaglia *et al*., 2018). However, early complete defoliations in maize have the potential to delay the period from planting to anthesis (Dungan and Gausman, 1951), silking (Battaglia *et al*., 2018), or both (Cloninger *et al*., 1974) by 2 to 8 days. On the other hand, low-intensity defoliation after the V10 stage could reduce the final yield by up to 30% (Battaglia *et al*., 2019a). From this point, damage in plants subjected to hail damage gradually increases, with grain yield reductions of up to 100% when defoliation occurs immediately before, at, or a few days after the VT stage (Hanway, 1969; Egharevba *et al*., 1976; Vasilas and Seif, 1985; Andrade *et al*., 1999; Adee *et al*., 2005). In previous studies, yield losses associated with defoliation around VT/R1 were mainly explained by reductions in kernel number (KN) (Culpepper and Magoon, 1930; Hanway, 1969; Severini *et al*., 2011; Tamagno *et al*., 2016; Battaglia *et al*., 2018), with most significant decreases in KN ranging between 62% and 95% (Egharevba *et al*., 1976; Battaglia *et al*., 2018). Grain yield losses due to hail damage can also be explained by reductions in the kernel weight (KW) when defoliation occurs immediately before or at R2 (beginning of the grain filling period) (Hanway, 1969; Egharevba *et al*., 1976; Tollenaar and Daynard, 1978; Echarte *et al*., 2006) without changing the final KN. However, more recent studies have also shown that decreases in KW with partial or complete defoliation around the R2 stage may decrease not only KW but also the final KN (Tamagno *et al*., 2016; Battaglia *et al*., 2018). Following completion of the critical period for grain yield determination (*i.e*., +/– 15 to 20 days bracketing VT/R1 stages), grain yield losses due to hail damage decrease progressively as maturity is approached (Eldredge, 1935; Vorst, 1993) to reach minimum values at or around 0% yield reduction when damage occurs around maturity (Dungan, 1934; Jenkins, 1941; Adee *et al*., 2005; Battaglia *et al*., 2018). Determination of the hail damage impacts on maize for biomass and silage purposes has received less attention than similar effects in maize for grain production (Simonelli *et al*., 1983; Lauer *et al*., 2004; Barimavandi *et al*., 2010). In a study conducted almost 50 years ago, Baldridge (1976) evaluated the effects of simulated hail damage on both forage yield and grain yield in irrigated areas in Montana, U.S., and found that defoliation (between 50 and 100%) conducted at V7 and V11 stages reduced forage yield more than the grain yield; on the contrary, when defoliations were applied at the V15, VT and R2 (*i.e*., milk stage), the reduction in the grain yield was greater than the concomitant

reduction in the forage yield. More recently, Lauer *et al*. (2004) found that a 16% decrease in yield occurred if 100% defoliation occurred at V7. The impact that different defoliation timing and severities have on final maize grain yield is utilised by the crop insurance industry to estimate the percentage of grain yield loss due to defoliation events (Österreichische Hagelversicherung, 2013). In the US, charts used by insurance companies to assess the maize grain yield loss due to defoliation at different stages and with different severities were developed in the late 1960s and are still valid in most situations (Battaglia *et al*., 2019a).

## Remote sensing and atmospheric events

Remote sensing is widely used in agricultural management to evaluate topographic and biophysical characteristics (Wang *et al*., 2019; Szantoi *et al*., 2020; Dindaroglu *et al*., 2021; Nutini *et al*., 2021). Optical data acquired from any distance from the ground (terrestrial, aerial, and satellite) has effectively estimated the extent of defoliation caused by hail in maize canopies (Gobbo *et al*., 2021). Moreover, these remote monitoring platforms could be used as a possible solution to drastically reduce the associated costs of insurance inspections in hail-damaged fields (Sosa *et al*., 2021). The image acquisition combined with field measurements carried out in a field survey could provide cost-effective scenarios to be used to map the extent and severity of defoliation of maize plants subjected to hail events (Erickson *et al*., 2004).

Another methodology found in the literature consists of directly evaluating hail defoliation using remote sensing images collected before and after the hail event through a simple difference in spectral indices (Prabhakar *et al*., 2019). The principle that guides the use of satellite imagery (visible or near-infrared) with change detection for the assessment of hail damage is that hail and wind can alter the characteristics of the canopy, producing changes in the vegetation structure that can be detected from the sensor (Prabhakar *et al*., 2019). At the experimental level, the combination of optical-infrared and microwave-radio wave data (data merge of two different satellites) can also be used to monitor large-scale hail events (Gallo *et al*., 2019; Molthan *et al*., 2020). The drawback of these technologies for small-scale farms is their inherently low spatial resolution, which can be unsuitable for highly fragmented agricultural landscapes. Using vegetation indices (VIs) as a single indicator quantifies and simplifies the understanding of one or several specific biophysical parameters of the crop (Schillaci *et al*., 2021). Historically, most VIs developed for crop yield prediction purposes are focused on large areas (Hamar *et al*., 1996; Sibley *et al*., 2014; Lopresti *et al*., 2015). With the increasing availability of satellite imagery and their temporal and spatial resolution (Lobell and Azzari, 2017; Azzari *et al*., 2017), medium to high-resolution optical sensors are helpful for agricultural monitoring applications (*e.g*., Planet, Landsat, RapidEye, and Sentinel). Sentinel-2 (S2) provides free and publicly accessible data, with a medium spatial resolution (10-20 m for the main spectral bands) and a high temporal resolution (5 days at the equator) (Drusch *et al*., 2012). The NDVI index (Rouse *et al*., 1973) is one of the most used VIs to evaluate crop growth and yield (Peralta *et al*., 2016), and becomes a reference point for researchers developing new VIs (Hatfield *et al*. 2008). However, NDVI can be subjected to saturation in mid-high leaf area index (LAI) conditions (Nguy-Robertson *et al*., 2012). Other issues regarding the use of the NDVI index were analysed by Jing *et al*. (2004). According to the literature, NDVI is sensitive to the concentration of chlorophyll, the humidity of the soil surface layers, the light diffused in the atmosphere, the angle of view zenith, and the zenith of the sun. The NDVI becomes less sensitive in these conditions but is also less susceptible to variation in vegetation parameters. Although this saturation may be partially contained when selecting the bands to be analysed, the best alternative is to use three-band indices (Verrelst *et al*., 2013, 2015). To overcome the saturation problem, new VIs have been developed (Fadaei, 2020; Talukdar *et al*., 2020; Leo *et al*., 2021). Verrelst *et al*. (2015) evaluated many vegetation indices generated from Sentinel-2 data and found that the best indices matched the three-band indices according to the normalised formula (ρ560- ρ1610- ρ2190) / (ρ560 + ρ1610 + ρ2190). According to Kang *et al*. (2016), EVI and EVI2 are the most effective among the various indices. The EVI-LAI and EVI2-LAI relationships are robust and valid in multiple spatial scales and global scales.

## Agricultural insurances

Insurance is one of the most widely used and recognised methods for managing the risk of potential losses due to severe weather events. Insurances are a passive protection method, as insuring does not prevent the risk of damage but allows compensation based on the damage received (Curry and Koczberski, 2012; Gaupp *et al*., 2017; Erhardt *et al*., 2019). Weather extremes can be categorised as catastrophic (infrequent, high impact) or non-catastrophic (frequent and low impact events) (Lyubchich *et al*., 2019). Cumulating losses yearly, even non-catastrophic events tend to cause more significant losses than natural disasters (Lesk *et al*., 2016); however, frequent and low-impact events do not receive considerably less attention from the media, public opinion, and scientific literature. Measuring the impact of non-catastrophic events is crucial in developing efficient weather risk mitigation strategies while raising public awareness of weather risks and improving society's resilience to the actual occurrence of these events (Toeglhofer *et al*., 2012; Toreti *et al*., 2019). For example, non-catastrophic weather risks can directly impact the increase in costs and the decrease in sales volume in agricultural companies (Capitanio and De Pin, 2018). High risks also imply more expensive insurance or even a denial of insurance coverage (Lyubchich *et al*., 2019). Every year, the Norwegian Meteorological Institute, in collaboration with the EASAC (European Academies Science Advisory Council), draws up a report on extreme weather events in Europe. Recently, one of these reports highlighted that the insurance sector recorded a sharp increase in the number of extreme weather events causing significant economic losses in Europe over the last four decades (Hov *et al*., 2013). For example, insurance companies in Austria spent 240 M EUR to compensate for agricultural losses due to extreme weather events in 2013 (Österreichische Hagelversicherung, 2013). These measures are necessary to reduce the impacts of abiotic stresses and weather associated with climatic change (Link *et al*., 2006; Shah *et al*., 2021). As mentioned before, a traditional field damage estimation process operated by insurance technicians and based on standard approaches can be expensive in terms of time, money, and difficulties accessing certain parts of the field. Moreover, the subjective nature of the field-taken measurements could compromise the efficiency and accuracy of the observations and, with this, the value of the resulting estimates. Innovative tools for precision agriculture monitoring would be helpful not only for the insurance sector but also for large-scale agriculture: damage mapping, for example, can provide vital information to improve agricultural management (Vescovo *et al*., 2016).

## Aims of the work

This work aims to evaluate the feasibility of remotely sensed vegetation indices to provide data relating to damage from atmo-

spheric agents (hail and wind) on the cultivation of grain maize and silage. The NDVI index and other indices (SAVI, MSAVI, MSAVI2, ARVI, MCARI) were used to obtain representative average values of the fields under study (with the exclusion of headlands) to evaluate the relationship between the index and the damage estimated by hail, strong wind or their combination.

Specifically, this study aimed to: i) evaluate whether it is possible to distinguish crops damaged by atmospheric events (*i.e.*, that have suffered damage greater than or equal to 10% of the gross production not-damaged crops (not subject to adverse weather conditions) and crops affected insignificantly (damage less than 10% of the gross production); ii) for the fields where ground damage was estimated, utilise satellite images to compare this information with the field estimation.

## Materials and methods

The study includes the comparison of two methodologies: i) damage assessment through field data collection and insurance damage evaluation tables; ii) damage estimation through VIs. Prior to that, an unsupervised classification on the VIs time series was carried out to distinguish between maize planting dates and type (grain or silage) (Figure 1).

### Study area and field data

Field data were collected in 125 sites in the Brescia district (Lombardy), Italy, during the spring and summer seasons in 2018. The plots had various sizes, ranging from one to eight ha (on average 4 ha), with less than 2-3% slope, and were always under either maize for grain or silage purposes. According to the Köppen classification, the bioclimate is Cfa class (temperate climates with humid summer and the average temperature of the hottest month above 22°C). The average 25-year annual rainfall in the area is 990 mm (ISPRA, 2020).

Cadastral information from the Italian Revenue Agency was then retrieved using the STIMATRIX for Maps tool (*formaps.it*). Through this platform, the Cadastral information was overlaid to Google Earth™. These fields were loaded via a polygonal vector layer in QGIS (version 2.18 and 3.10). The Italian Cadastre was used for their univocal identification: each field was named with the specific (Sheet, Map, Municipality) to make the files unique and easy to understand. As a result, each specific map within a sheet of a municipality in the Italian Cadastre is unique.

The FAO class of the crop, the hybrid, is declared by the farmer when this crop was damaged by atmospheric events (hail, strong wind, *etc.*), and agricultural insurance technicians estimate the percentage of damage.

Thanks to the technical assessment of the damage compiled by a professional technician from an accredited agricultural insurance company (data provided for this research for scientific purposes only), the damage reports of the 125 plots were recovered to assess the degree of damage after the hail event to estimate the projected yield damage. All personal information has been omitted for privacy reasons. In addition, the data collected for this analysis were granted solely for scientific purposes; therefore, personal data and coordinates of the fields have been omitted.

For each field under study, the percentage of product loss that the insurance technicians identified and the actual damage at the survey date were reported. The *loss of product* expression means that: i) the grain is no longer suitable when intended for grain maize; ii) a quantity of forage and quality of residual forage can no longer be obtained when intended for silage maize.

### Unsupervised classification for crop type mapping

We performed K-means unsupervised learning to cluster VIs data into maize types using SNAP (ESA). K-means is a commonly used unsupervised classification algorithm (Ma *et al*., 2020). K-means partitions m samples into K clusters by alternately assigning samples to the nearest cluster centroid, measured by Euclidean distance. Then, the cluster centroids are updated using the mean of the samples assigned to the cluster (Xiong *et al*., 2017).

A single raster image was obtained for each plot (no. 125), for each scene (no. 39), and each vegetation index (no. 6), for a total of 29,250 images. Therefore, it is possible to analyse the pixels of these images using change detection (value of the pixel calculated

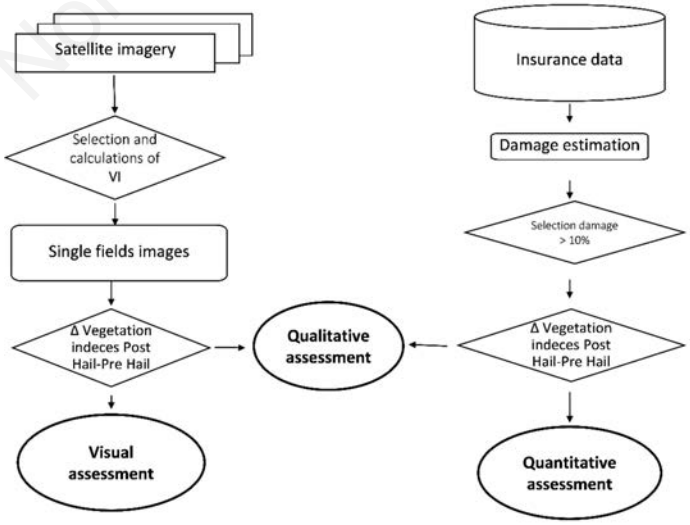


**Figure 1. Methodological workflow. VI, vegetation index.**

as T1-T0) or by evaluating the change in the vegetation index per pair of temporally contiguous images. Furthermore, given that maize cultivation and its management vary according to the anthropogenic element, soil conditions, and weather, an unsupervised classification by K-means was carried out to identify sets of homogeneous crops.

To make three clusters (crop of silage maize, second crop maize and early-sown maize from grain), the square root of the sum of the analysed fields (rounded up) was set, and 22 measurements between 04/24/18 and 08/20/18 as variables. This procedure was carried out to reduce the classification errors that would occur using dates before 19/04/18 or after 30/08/18 and to sort the data, displaying the trend of the indices of each cluster and then eliminating any anomalies from the total. The maximum number of iterations was 999, and the convergence criterion was 0. In addition, the *use moving averages* option has been added, and cluster indexing as a final result.

Therefore, sorting is carried out, and some fields of the clusters are excluded. The sum of the land cleared of anomalies is 117 (for the NDVI index). Then, K-means carries out a new classification, and the computer is instructed to classify three classes: the early-sown maize from grain, the early-sown silage maize, and the late-sown maize. This procedure was carried out for each vegetation index.

## Operating guidelines for the insurance damage assessment

In Italian agricultural insurance, various methods exist to estimate the damage caused by hail (Capitanio and De Pin, 2018; Vroege and Finger, 2020; Vyas *et al*., 2021). Among them, the most used by the insurance companies are based on a visual assessment of the field and the field survey and collection of a few samples of leaves that have been subjected to the damage and compare them with a scale of projected yield losses. Here, a methodology has been used that quantifies the damage from atmospheric adversities on maize by analysing the foliar inefficiency. Foliar inefficiency could be defined as the reduction in the functionality and ability of the plant to normally perform the functions of photosynthesis, respiration, and transpiration and does not correspond to the defoliation suffered by the plant. During the appraisal phase for the assessment of defoliation damage, technicians from insurance companies recorded a series of parameters, such as the identification of the plots, the vegetative state of the damaged crop, and the possible presence of diseases or damages that cannot be compensated, among others. At this phase, technicians use different tables and graphs that relate the loss of leaf (*i.e*., defoliation severity) at a specific growth stage (*i.e*., defoliation timing), and its consequent inefficiency, with a decrease in grain or biomass production. These tables are/were then used in a methodological context that allows/allowed to relate other elements that compete to determine the actual damage: direct damage to the tassel, direct or indirect damage to the ear, malformations, *etc*. An example of a typical table used by Italian insurance companies is shown in Figure 2, step 3. In this assessment methodology, maize plants can be classified as non-damaged, moderately damaged, and severely damaged. There is a reference to the number of plants sampled and the percentage of damage the technician assigns to each portion of the plant sampled (leaves, the stalk, and the kernels). With a simple



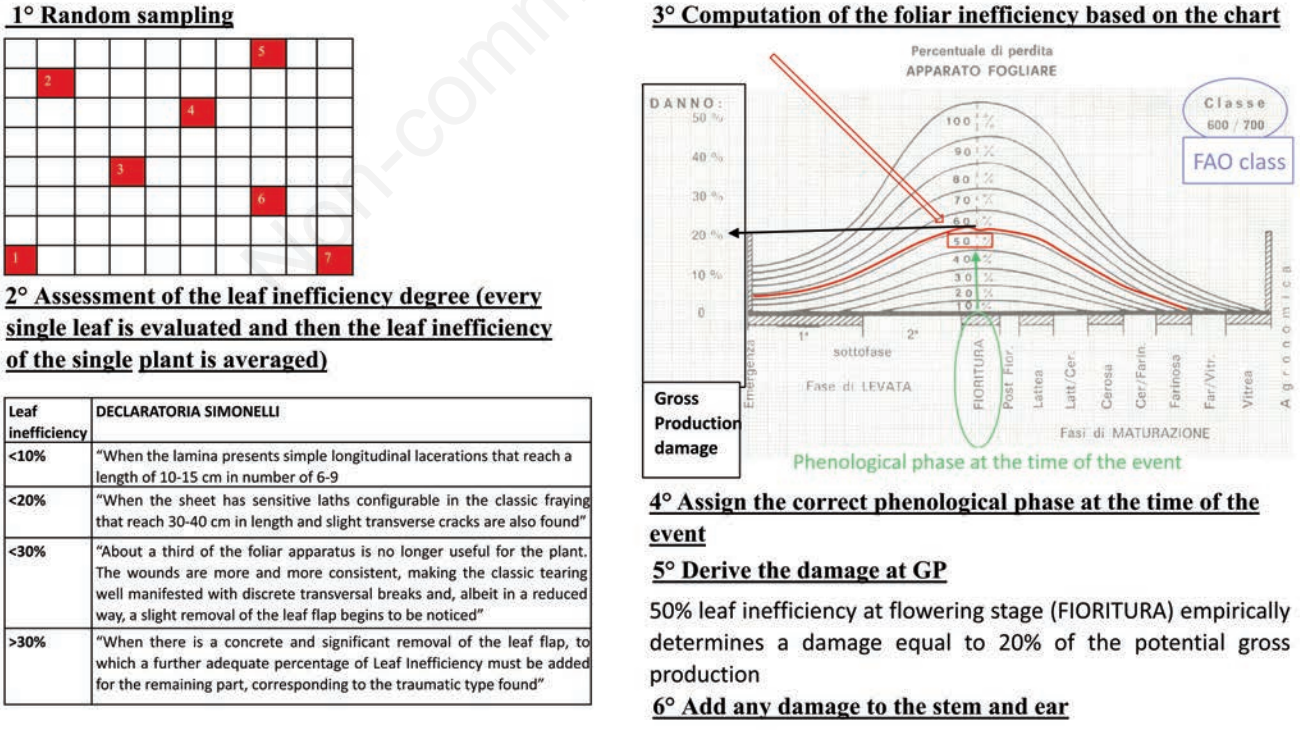


**Figure 2. Estimation of the damage caused only by the inefficiency of the photosynthetic apparatus to the phenological stage. GP, gross production.**

weight average from randomly taken (Figure 2, step 1), and representative plants of the non-damaged, moderately damaged, and severely damaged populations, the technician can obtain good estimates of field damage percentage. The determination of the damage rate attributed to the 'leaves' component derives from the estimate of the percentage of loss of the foliar apparatus carried out by the technician. The latter, with his own experience or with the help of additional equipment assesses all the leaves in the maize plant and then attributes an overall average percentage of damage to the photosynthetic apparatus of the particular plant under observation. The operation is then repeated in several neighbouring plants that are to be randomly chosen, and an estimated average percentage of damage is defined for the entire plot or field under analysis. The calculated damage percentage is related using empirical tables with the inefficiency of the photosynthetic apparatus in relation to the phenological stage in which the crop was at the time of the hailstorm or adverse event can be seen in Figure 1.

The damage to the stem is closely related to the damage to the leaves, corresponding to a percentage of leaf damage. In contrast, the damage to the kernels can be direct (loss of kernel or a part of the ear by the direct impact of hail) or indirect (*e.g.*, increase in the % of abortion or unfertilized kernels hit by hail). In Figure 2 of the supplementary materials, it is possible to consult where individual leaves of the maize plant for which a percentage of foliar inefficiency has been attributed according to the *Declaratoria Simonelli*, a document dated back to 1978, can be observed as reported in step 2 of Figure 2.

Some insurance companies (*e.g.*, the company that provided the data) use this methodology to estimate the production losses of grain maize. Concerning silage maize, there is the assessment of an increase in damage due to the loss of forage quality. This increase is tabular and corresponds to a certain percentage of damage based on the damage attributed to the grain. Table 1 shows how this quantification of quality loss occurs in an Italian agricultural insurance company.

In Table 1, the first two lines identify the percentage of damage (percentage of the biomass lost) and the quality loss coefficient (an empiric coefficient used by the insurance to calculate the indirect damage, potential pathogen attacks, and reduced resilience of the plants) to be applied to the residual biomass after the hailstorm in the field for the determination of the quality damage of the silage maize.

## Vegetation indices calculation for damage assessment

The Sentinel-2 program is part of the Global Monitoring for Environment and Security (GMES) program. In fact, Sentinel-2 contains a multi-spectral imager (MSI) sensor that allows a maximum amplitude of 290 km to record 13 spectral bands reflected from the earth's surface. These bands range from visible light to short wave infra-red SWIR short infrared with different spatial resolutions: i) 10 meters for visible light and NIR; ii) 20 meters for the red-edge bands and SWIR; iii) 60 meters for the bands that allow the atmospheric correction of the data.

The average temporal resolution of the Sentinel-2 is five days. For a multi-temporal analysis, it is common to disregard some images due to the high cloud cover that limits vegetation's detection. In this work, the images were downloaded from the ESA server at the site http://scihub.copernicus.eu/. The survey period has been set between 01/03/18 and 01/10/18. Sentinel-2 images are geometrically corrected by top-of-atmosphere reflectance (TOA) or by the variations caused by the atmosphere with TOC (top-of-canopy reflectance). The L1C and L2A processing levels imagery is downloadable from Sentinel Open Hub.

An automatic sorting based on the estimated percentage of cloud cover has not been applied to avoid running into the following problems: i) the inexistence of a well-defined threshold (threshold) that would allow the images to be classified before their use; ii) the elimination of useful images due to the position of the cloud cover concerning the position of the land analysed in the image: paradoxically, an image with high cloud cover may not affect the areas analysed or vice versa. This way, 39 scenes for S2A and 35 scenes for S2B in the Brescia District were selected. Using GIS software, a second visual selection significantly decreased the usable scenes.

The raw images downloaded from the Open Access Hub site are not readily usable: they contain the 13 spectral bands detected by the MSI sensor, but each of them is structured according to its spatial resolution does not allow for the immediate creation of VIs. Therefore, sentinel application platform (SNAP) software, developed by ESA with the primary purpose of processing Sentinel-2 data, has been used to process the downloaded Sentinel-2 images. Versions 8.0.0 has been used. Using SNAP, the raw image downloaded from Open Access Hub was resampled to bring all the bands produced by Sentinel-2 back to the same spatial measurement unit. It was decided to resample each spectral band back to a spatial resolution of 10 m. Subsequently, six different vegetation indices are calculated using the SNAP software (NDVI, SAVI, MSAVI, MSAVI2, ARVI, MCARI).

## Damage estimation from vegetation indices

The images of the indexes of the plots are processed through the QGIS software. Only the scenes before (PRE) and after (POST) of hailstorm events were selected, and a new layer was calculated as VI POST-VI PRE (ΔVI) is the difference between the index of the POST event and the PRE -EVENT vegetation index. A colour scale based on five quantile classes is created for each image to classify each pixel into one of the five classes (Xiong *et al*., 2017).

In addition to the verification of the change detection through vegetation indices and the estimation of the accuracy of the satellite data compared with the ground data, this work also aims to identify and evaluate the relationship between the difference (ΔVI) and the damage on the gross production reduction recorded on the ground to assess the possible relationship. The procedure for identifying and evaluating the relationship between ΔVI and ground damage is as follows:

ΔVI values are grouped by event: this is due to the phenology of maize, which changes over time; damage to the ground equal to

**Table 1. Quality damage, only for silage maize and derived percentages of damage.**

| % of damage observed in production | % Quantity loss | 0 | 10 | 20 | 30 | 40 | 50 | 60 | 70 | 80/100 |
|---|---|---|---|---|---|---|---|---|---|---|
| | Coefficient of quality loss per residue of % of quantity loss | 0 | 4 | 6 | 8 | 15 | 20 | 25 | 30 | 40 |

0% is assigned to not-damaged and to those affected by damage less than 5% (average between 0 and 10) only if they are not given a precise value; since there were five different hail events, the response in terms of VIs needs to be normalised. The difference VIs data is transformed into a z-value according to the formula:

$$\frac{x_i - \mu_j}{\sigma_j} \quad (1)$$

where $x_i$ represents the *i-th* value that the vegetation index assumes according to the space-time information (plot and data detection date), $\mu_j$ is the *j-th* average of the vegetation index on the temporal basis (detection date), and $\sigma_j$ is the *j-th* standard deviation of the vegetation index on a time basis (Bell *et al*., 2020). This procedure aims to normalise the data and allows the comparison between multiple atmospheric events despite the diversity of distribution of the index values. Once the z values have been created, we use three methods and compare the results with three different accuracy calculations.

The first method analyses the data regardless of the crop's phenological stage and the dates of atmospheric events. In this case, the analysis focuses on all the data. The second method analyses the data regardless of the phenological stage, but five separate analyses are carried out considering the individual atmospheric events. Finally, the third method analyses the data considering the different events and the different phenologies of the crops: ten additional analyses are carried out.

To evaluate the accuracy of the methods, the MS Excel 'Solver' tool is set to determine the most convenient threshold to maximize the overall accuracy (Congalton 1991), the probability of false alarms, and the probability of missed alarms. For calculating these last two accuracies, their sum is considered, *i.e*., the threshold that determines the lower of the values of the combinations is selected (false alarm + missed alarm). To choose the left and right limit of the curve, which the threshold calculated by the solver instrument must not exceed, this limit is set in ±2σ of the analysed data. This evaluation approach is often used in assessing remote sensing classifications, for crop type mapping (Vuolo *et al*., 2018), and direct assessment of yield losses (Furlanetto *et al*., 2021).

Overall accuracy: $\frac{TP+TN}{TP+TN+FP+FN}$

Incorrect detection: $\frac{FP}{TP+FP}$

No detection: $\frac{FN}{TN+FN}$

where TP, true positives; TN, true negatives; FP, false positives; FN, false negatives.

## Results

### Unsupervised classification of grain maize and forage maize

The K-means unsupervised classification allowed the classification of all the fields considered in three clusters in this analysis. The fields affected by atmospheric adversities are then considered for the change detection analysis. In Table 2, the results of the cluster analysis are presented (Figures 3 and 4).

### Accuracy of the change detection method

A sampling of the majority component was performed to analyse the data in a balanced way. A K-means algorithm selected representative centroids of the not-damaged fields, reducing them

**Table. 2 Number of cases (fields number) in each cluster.**

| Class | | No. of individual fields |
|---|---|---|
| Class | 1 | 18 |
| Class | 2 | 24 |
| Class | 3 | 75 |
| Correctly classified | | 117 |
| Missing | | 0 |

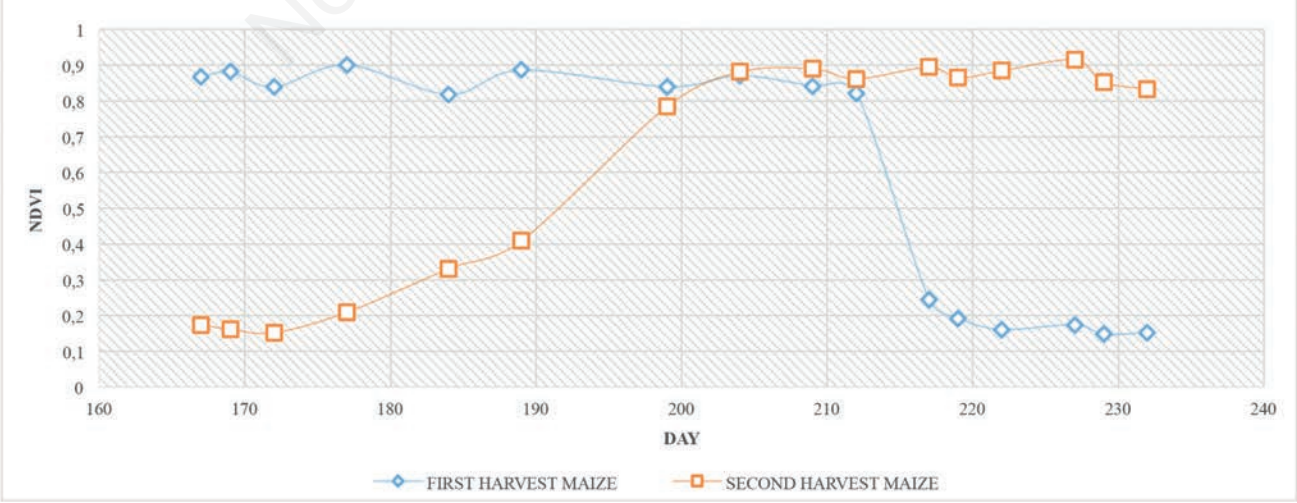


**Figure 3. Typical normalized difference vegetation index (NDVI) pattern of the early sown maize (blue dots) and late maize for silage (orange dots).**

from 550 total during the five events to 37. Considering the same area for each class shown in Table 3, by randomly choosing a sample area of an unaffected crop by damages, it is possible to perform the accuracy calculations on a balanced sample (*e.g.*, for the silage maize 1st sowing period 26 ha of unaffected areas were considered to perform the accuracy analysis). Table 4 shows the ranking of the VI in terms of accuracy and false-positive discovery. The MSAVI index ranks first among the other VIs with an overall accuracy of 73.3%, while the NDVI ranks last with 65.3%. The result of the accuracy calculation of the VIs showed the highest accuracy with soil-adjusted indices, *i.e.*, the indices that reduce the noise produced by the soil (SAVI, MSAVI, MSAVI2). These indices have shown the greatest accuracy against ground truth, minimising false positives and false negatives. The difference in accuracy between

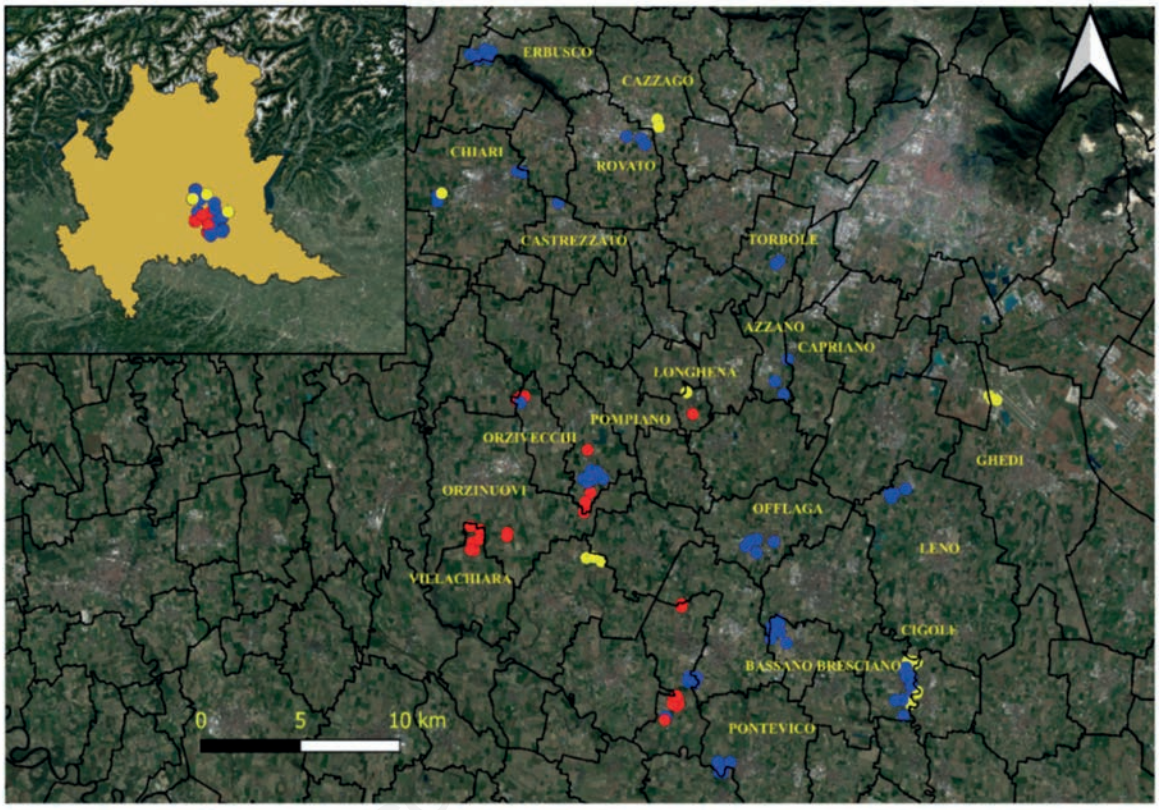


**Figure 4. Classification of the maize cultivated in the study area plots, blue dots represent early-sown corn for grain production, red dots are late-sown maize, and yellow dots are early-sown maize for silage.**

**Table 3. Assessment of the fields affected by damage.**

| Class | No. of fields (area) | No. of fields (area affected by damages) |
|---|---|---|
| 1 Silage maize 1st sowing period | 18 (78 ha) | 7 (26 ha) |
| 2 Silage maize 2nd sowing period | 24 (94 ha) | 10 (41 ha) |
| 3 Corn 1st sowing period | 75 (220 ha) | 22 (69 ha) |
| Total | 117 (392 ha) | 39 (136 ha) |

**Table 4. Accuracy of the vegetation indices change detection (127 fields).**

| Index | Event no. | Overall accuracy | False positive-false negative range |
|---|---|---|---|
| MSAVI2 | 01->05 | 72.0% | 48.6% |
| SAVI | 01->05 | 70.7% | 47.2% |
| MCARI | 01->05 | 65.7% | 45.6% |
| NDVI | 01->05 | 65.3% | 47.9% |
| ARVI | 01->05 | 66.7% | 47.2% |
| MSAVI | 01->05 | 73.3% | 46.5% |

Fabijańczyk and Zawadzki, 2022. MSAVI2, modified soil-adjusted vegetation index; SAVI, soil-adjusted vegetation index; MCARI, modified chlorophyll absorption in reflectance index; NDVI, normalized difference vegetation index; ARVI, atmospherically resistant vegetation indexexplain; MSAVI, modified soil-adjusted vegetation index.

the MSAVI index and the NDVI index, *i.e.*, the maximum difference between the two indices equal to 8.0%, corresponds to 6 out of 75 fields (not damaged or damaged), which the NDVI index places among false positive/false negatives while the MSAVI index places between true positive/true negative. Maps of the MSAVI index are displayed in Figure 5 and Table 5.

A set of fields increased their VIs and the vegetation within-field variability after the hailstorm event due to a marked decrease in the areas damaged by the hailstorm; therefore, a slightly lower detection rate was observed from the VI change detection method in the first and second event, from the third event to the fifth, the assessment of damage was very similar between insurance surveys and VIs change detection (Figure 6).

By analysing all the images (117), it was possible to assess three different ways in which the MSAVI index behaves in *damaged* fields: i) partial decline, *i.e.*, the VIs drops only in a part of the land. Therefore, it is assumed that the land has been damaged, especially in parts showing the greatest decline; ii) generalized decline, *i.e.*, the VIs falls widely over the entire plot. It is assumed that the field has been homogeneously damaged; iii) no decline or the VIs varies insignificantly. This is the most controversial case: it determines any False Negatives when a method based on the POST-PRE difference of a vegetation index is used. Using the MSAVI and the 35 images of damaged fields, it was possible to group images into the three scenarios mentioned above. Therefore, we obtained nine scenes in which the MSAVI decreased partially, 13 scenes in which the MSAVI fell homogeneously, 13 scenes in which the MSAVI did not decrease significantly.

## Discussion

### Crop type classification

To classify grain maize and forage maize, the unsupervised classifications allowed for the crop mask's definition. The classification approach consisted of two steps: i) the first to process the raw data and exclude any anomalies upstream of the processing; ii) the second to classify types of the same crop (early-sown, late-sown, grain, silage maize).

**Table 5. Modified soil-adjusted vegetation index and normalized difference vegetation index score in true positive, true negative, false positive, and false negative accuracy.**

| Index | TP | TN | FP | FN |
|---|---|---|---|---|
| MSAVI | 25 | 30 | 7 | 13 |
| NDVI | 17 | 32 | 5 | 21 |

MSAVI, modified soil-adjusted vegetation index; NDVI, normalized difference vegetation index; TP, true positive; TN, true negative; FP, false positive; FN, false negative.



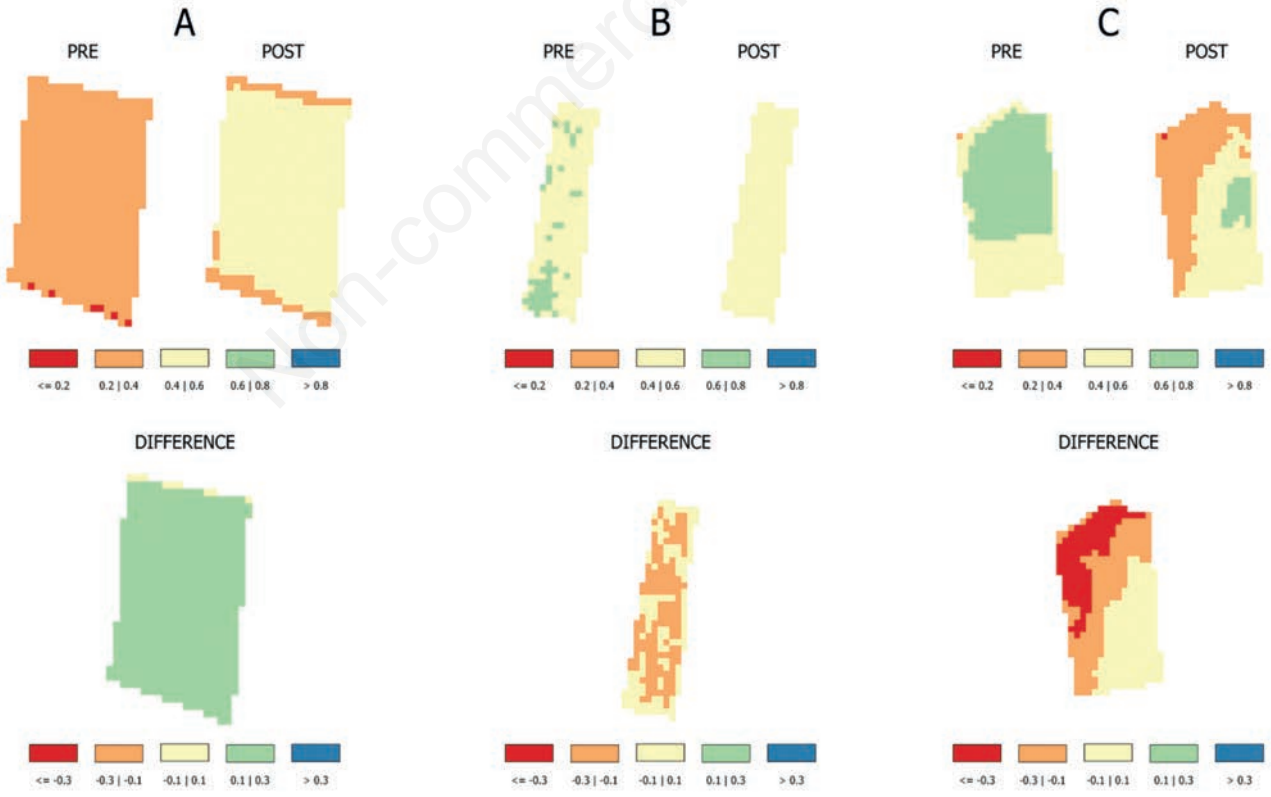


**Figure 5. A) Pompiano field 17;32; B) Verolavecchia field 4;12-14-15; C) Orzinuovi field 25;133-134-135-136. Within each image, three representations of the vegetation index (VI) can be identified on the top before (PRE) and after (POST), while on the bottom the variation of the VI as difference POST-PRE (ΔVI). Showing the variation of the modified soil-adjusted vegetation index only for three responses after the hailstorm i) decrease in the VI, no significant changes in VIs conditions, and VIs increase after the hailstorm.**

Concerning the first step, the visual analysis of the deleted images, two anomalies of the VI are characterised: i) the presence in the plot of a different crop than maize and which is characterised by a variation of its own VIs; ii) the presence in the same plot of two different crops, one of which could be maize, which has different vegetative cycles and soil cover and which, by averaging all the pixels of the plot, produce distorted index data.

The second unsupervised classification was made to differentiate *a priori* the two patterns that occur in any index and distinguish, regardless of atmospheric events, early-sown and late-sown maize. However, the optimal classification was in three classes. The approach enabled us to distinguish between early and late-sown maize for grain or silage production.

## Calculation of the accuracy using the qualitative method

The comparison of the PRE, POST and ΔVI images of the damaged fields allowed us to identify three groups: i) the first is when the VI dropped down after the hailstorm on the part of the plot; ii) the homogeneous decline of the VI after the hail event throughout the plot; iii) no drop of the VI across the plot.

A simple spatial analysis of the variation of the VIs images, considering the fields that show a significant reduction in the index as damaged, cannot be the correct solution to determine any damage suffered by the crops.

An alternative solution could be using a finer ranking of the VIs to identify a possible variation in more detail (in the following work, the MSAVI has been classified into five classes of the size of 0.2 as the VI ranges from 0 to 1). However, this method also applied to not-damaged or only HIT land would increase false positives as they would be classified as significant small changes in the VI.

## Scientific interest in the results obtained and the novelty of the proposal

In the field of agricultural insurance, the most common method to estimate the damage produced by hail consists in first determining the percentage of observed hail-related damage in randomly selected and representative plants at the field level, to then relate these losses with the percentage of damage for a particular maize growth stage in the chart grain yield losses used by insurers (Lauer *et al*., 2004; Gobbo *et al*., 2021). However, using this method to determine the field damage following a hail event accurately is complex. Choosing representative plants subjected to hail damage can be time-consuming and overly subjective (Battaglia *et al*., 2019). Usually, hail-related damage in a field follows an irregular pattern within the field due to the different topography, the direction of the winds that displaced the hail during the storm event, and the randomness with which this has affected the crop. Furthermore, affected parts of the plot could be inaccessible, or the presence of a tall and well-developed crop could prevent the canopy from being seen in depth (Erickson *et al*., 2004). Operational problems arise in proceeding with this methodology.

The proposed method allows classifying an area with good accuracy, highlighting not only the differences between crops but also within it, exponentially increasing the information detail that can be obtained. The benefits of such methodology substantially

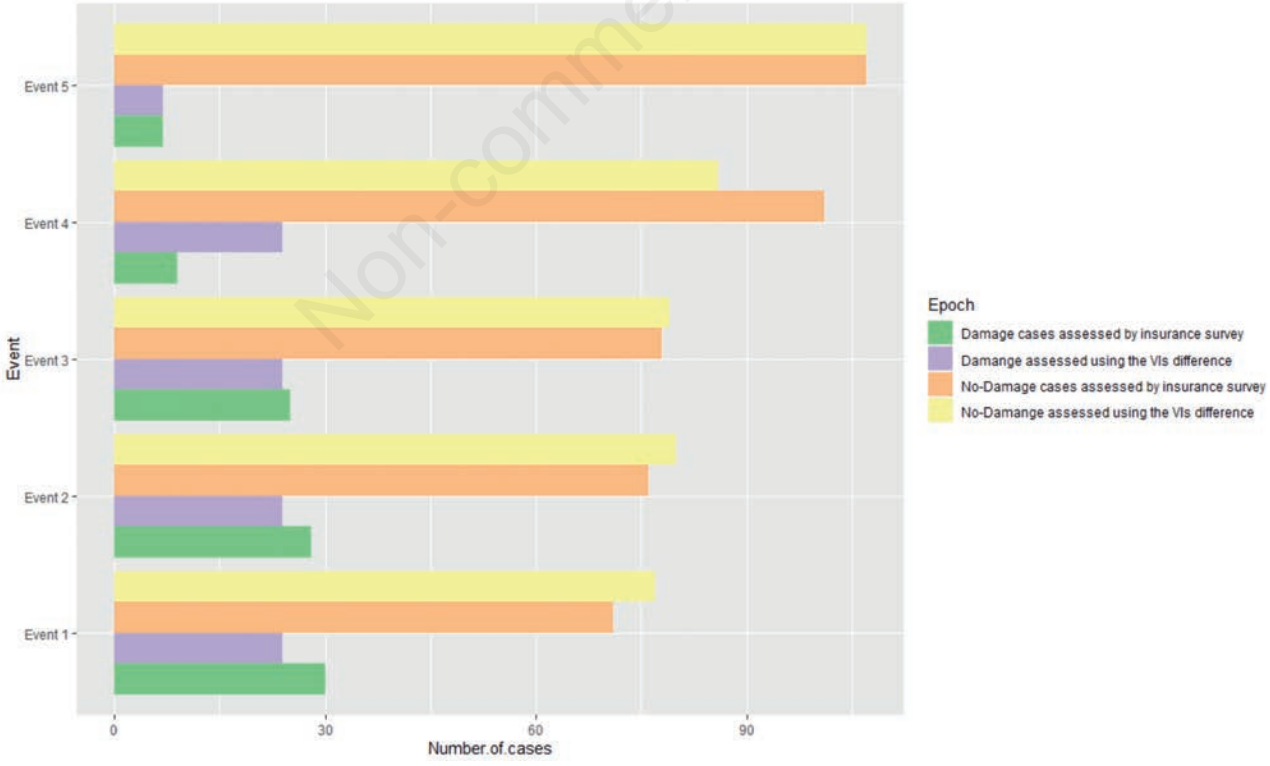


**Figure 6. Damage assessment via insurance survey and vegetation index (modified soil-adjusted vegetation index difference after-before the hail event).**

impact the farmers to understand better how an atmospheric event may have damaged their farm. From the advisor's point of view, the methodology has allowed defining which parcels have been damaged by a weather event that has just passed or evaluating data from previous years. For a better management strategy during the cultivation, the methodology can indicate minor damage and adjust N fertilisation and irrigation. The economic advantages of the methodology can bring some innovation in the agricultural insurance companies and their providers to better organise their human resources and develop a *sampling map* for further detailed on-ground assessment. The more accurate detection of damages will be useful for defence consortia (*e.g.*, *Confagricoltura*) to assess the damage at a district level and intervene alongside farmers. Finally, local and national public entities can benefit from adopting the methodology as a forecasting and verification tool.

### Possible future developments

It was possible to evaluate some limitations during the work mainly due to reliable damage estimation done in a scientific context out of economic interests. It is expected that future investigations will take advantage of the information from this work and may enhance some aspects that could not be investigated, such as the measurement of a set of biophysical variables on the ground (wet biomass, dry biomass, chlorophyll content, quantity of water in the canopy) as well as the comparison with the satellite data. The use of other methods, such as the combined reflectance of the main spectral bands and wavelengths (blue, green, red, NIR, SWIR). The increase of the initial samples in other regions and additional years. The use of balanced data provided a better view of the phenomenon. Furthermore, it allowed us to improve the discovery rate of damaged fields, *i.e.*, the definition of some parcels damaged in the same way (*e.g.*, 20 fields at 0% damage, 20 fields at 5% damage, 20 fields at 10% damage, *etc.*). Using satellite or unmanned aerial vehicles (*e.g.*, drones) data at a higher spatial resolution can improve the automatic delimitation of the plots, especially when a reduced surface or an irregular perimeter characterises them.

Finally, it would be interesting to quantify the costs of applying the methodology and the development of an automated workflow considering the market interests considering each stakeholder involved.

## Conclusions

The significant and recent increase in the number of claims to agricultural insurance companies in many areas of the planet has spurred an interest in the potential use of innovative tools to cope with this situation. Improved monitoring tools can provide strategic information for planning adaptation measures in the agricultural and forestry sectors.

In this work, vegetation indices (SAVI, MSAVI, MSAVI2, ARVI, MCARI) have been identified and evaluated to classify the damage produced by some atmospheric agents (hail and strong wind) using scenes obtained from the Sentinel-2 satellite fleet.

The results achieved are: i) in evaluating the indices from the qualitative point of view of the damage classification, *i.e.*, the accuracy in correctly distinguishing damaged soil from not-damaged, the vegetation indices of the 'soil-adjusted' type proved to be the most efficient. Among them, the MSAVI index stands out as the most performing of the six tested indices; ii) the images of damaged fields can be classified into three groups: partial decline in the index, homogeneous decline, and no decline. While the first two cases are strictly associated with damaged fields, the third case can be easily confused with the images of not-damaged fields and, therefore, depending on the method, is subject to being false negative; iii) Sentinel-2's decent time resolution allows for numerous scenes with good spatial detail, but most images need to be filtered due to cloud cover; iv) the damage estimates carried out by third-party technicians tend to be approximate, and their assessment does not always reflect reality, due to estimation errors and the use of typical practices of the agricultural insurance sector.

## References

Abendroth LJ, Elmore RW, Boyer MJ, Marlay SK, 2011. Corn growth and development. PMR 1009. Iowa State University Extension, Ames, IA, USA.

Adee EA, Paul LE, Nafziger ED, Bollero GA, 2005. Yield loss of corn hybrids to incremental defoliation. Online. Crop Manage. 4:1-9.

Adnan M, Fahad S, Zamin M, Shah S, Mian IA, Danish S, Zafar-ul-Hye M, Battaglia ML, Naz RMM, Saeed B, Saud S, Ahmad I, Yue Z, Brtnicky M, Holatko J, Datta R, 2020. Coupling phosphate-solubilizing bacteria with phosphorus supplements improve maize phosphorus acquisition and growth under lime induced salinity stress. Plants 9:900.

Andrade FH, Vega C, Uhart S, Cirilo A, Cantarero M, Valentinuz O, 1999. Kernel number determination in maize. Crop Sci. 39:453-9.

Azzari G, Jain M, Lobell DB, 2017. Towards fine resolution global maps of crop yields: testing multiple methods and satellites in three countries. Remote Sens. Environ. 202:129-41.

Battaglia M, Lee C, Thomason W, Van Mullekom J, 2019. Effects of corn row width and defoliation timing and intensity on canopy light interception. Crop Sci. 59:1718-31.

Berti A, Maucieri C, Bonamano A, Borin M, 2019. Short-term climate change effects on maize phenological phases in northeast Italy. Ital. J. Agron. 14:222-9.

Botzen WJW, Bouwer LM, van den Bergh JCJM, 2010. Climate change and hailstorm damage: Empirical evidence and implications for agriculture and insurance. Resour. Energy Econ. 32:341-62.

Capitanio F, De Pin A, 2018. Measures of efficiency of agricultural insurance in Italy, Economic evaluations. Risks 6:126.

Childs SJ, Schumacher RS, Demuth JL, 2020. Agricultural perspectives on hailstorm severity, vulnerability, and risk messaging in Eastern Colorado. Weather Clim. Soc. 12:897-911.

Congalton RG, 1991. A review of assessing the accuracy of classifications of remotely sensed data. Remote Sens. Environ. 37:35-46.

Curry GN, Koczberski G, 2012. Relational economies, social embeddedness and valuing labour in agrarian change: an example from the developing world. Geogr. Res. 50:377-92.

Drusch M, Del Bello U, Carlier S, Colin O, Fernandez V, Gascon F, Hoersch B, Isola C, Laberinti P, Martimort P, Meygret A, Spoto F, Sy O, Marchese F, Bargellini P, 2012. Sentinel-2: ESA's optical high-resolution mission for GMES operational services. Remote Sens. Environ. 120:25-36.

Erhardt R, Bell J, Blanton B, Nutter F, Robinson M, Smith R, 2019. Stronger climate resilience with insurance. Bull. Am. Meteorol. Soc. 100:1549-52.

Erickson BJ, Johannsen CJ, Vorst JJ, Biehl LL, 2004. Using remote sensing to assess stand loss and defoliation in maize.

Photogramm. Eng. Remote Sens. 70:717-22.
EUROSTAT, 2021. Statistics | Eurostat. In: Crop Prod. Available from: https://ec.europa.eu/eurostat/databrowser/view/APRO_CPNH1__custom_1271804/default/line?lang=en Accessed: 8 September 2021.
Fabijańczyk P, Zawadzki J, 2022. Spatial correlations of NDVI and MSAVI2 indices of green and forested areas of urban agglomeration, case study Warsaw, Poland. Remote Sens. Appl. Soc. Environ. 26:2352-9385.
Fadaei H, 2020. Advanced land observing satellite data to identify ground vegetation in a juniper forest, northeast Iran. J. For. Res. 31:531-9.
Furlanetto J, Ferro ND, Briffaut F, Carotta L, Polese R, Dramis A, Miele C, Persichetti A, Nicoli L, Morari F, 2021. Mapping of hailstorm and strong wind damaged crop areas using LAI estimated from multispectral imagery. In: Precision agriculture '21. Wageningen Academic Publishers, The Netherlands, pp 315-321.
Gallo K, Schumacher P, Boustead J, Ferguson A, 2019. Validation of satellite observations of storm damage to cropland with digital photographs. Weather Forecast 34:435-46.
Gaupp F, Pflug G, Hochrainer-Stigler S, Hall J, Dadson S, 2017. Dependency of crop production between global breadbaskets: a copula approach for the assessment of global and regional risk pools. Risk Anal. 37:2212-28.
Gobbo S, Ghiraldini A, Dramis A, Dal Ferro N, Morari F, 2021. Estimation of hail damage using crop models and remote sensing. Remote Sens. 13:2655.
Grotjahn R, 2021. Weather extremes that affect various agricultural commodities. In: Extreme Events and Climate Change. Wiley, pp 21-48
Hamar D, Ferencz C, Lichtenberger J, Tarcsai G, Ferencz-Árkos I, 1996. Yield estimation for corn and wheat in the Hungarian Great Plain using Landsat MSS data. Int. J. Remote Sens. 17:1689-99.
Hatfield JL, Gitelson AA, Schepers JS, Walthall CL, 2008. Application of spectral remote sensing for agronomic decisions. Agron. J. 100:0370c.
Hov Ø, Cubasch U, Fischer E, Höppe P, Iversen T, Kvamstø NG, Kundzewicz ZW, Rezacova D, Rios D, Duarte Santos F, Schädler B, Veisz O, Zerefos C, Benestad R, Murlis J, Donat M, Leckebusch GC, Ulbrich U, 2013. Extreme weather events in Europe: preparing for climate change adaptation. Report produced by Norwegian Meteorological Institute in cooperation with EASAC. Available from: http://www.easac.eu/fileadmin/PDF_s/reports_statements/Extreme_Weather/Extreme_Weather_full_version_EASAC-EWWG_final_low_resolution_Oct_2013f.pdf
Johnson RR, 1978. Growth and yield of maize as affected by early-season defoliation 1. Agron. J. 70:995-8.
Lauer JG, Roth GW, Bertram MG, 2004. Impact of defoliation on corn forage yield. Agron. J. 96:1459-63.
Leo S, Migliorati MDA, Grace PR, 2021. Predicting within-field cotton yields using publicly available datasets and machine learning. Agron. J. 113:1150-63.
Lesk C, Rowhani P, Ramankutty N, 2016. Influence of extreme weather disasters on global crop production. Nature 529:84-87.
Link J, Graeff S, Batchelor WD, Claupein W, 2006. Evaluating the economic and environmental impact of environmental compensation payment policy under uniform and variable-rate nitrogen management. Agric. Syst. 91:135-53.
Lobell DB, Azzari G, 2017. Satellite detection of rising maize yield heterogeneity in the U.S. Midwest. Environ. Res. Lett. 12:014014.
Lopresti MF, Di Bella CM, Degioanni AJ, 2015. Relationship between MODIS-NDVI data and wheat yield: a case study in Northern Buenos Aires province, Argentina. Inf. Process Agric. 2:73-84.
Lyubchich V, Newlands NK, Ghahari A, Mahdi T, Gel YR, 2019. Insurance risk assessment in the face of climate change: Integrating data science and statistics. WIREs Comput. Stat. 11:1462.
Ma Z, Liu Z, Zhao Y, Zhang L, Liu D, Ren T, Zhang X, Li S, 2020. An unsupervised crop classification method based on principal components isometric binning. ISPRS Int. J. Geo-Inf. 9:648.
Meier U, Bleiholder H, Buhr L, Feller C, Hack H, Heß M, Lancashire PD, Schnock U, Stauß R, van den Boom T, Weber E, Zwerger P, Peter Zwerger C, 2009. Das BBCH-System zur Codierung der phänologischen Entwicklungsstadien von Pflanzen - Geschichte und Veröffentlichungen. J. Kult. 61:41-52.
Molthan AL, Schultz LA, McGrath KM, Burks JE, Camp JP, Angle, K, Bell JR, Jedlovec GJ, 2020. Incorporation and use of earth remote sensing imagery within the NOAA/NWS damage assessment toolkit. Bull. Am. Meteorol. Soc. 101:E323-40.
Nguy-Robertson A, Gitelson A, Peng Y, Viña A, Arkebauer T, Rundquist D, 2012. Green leaf area index estimation in maize and soybean: combining vegetation indices to achieve maximal sensitivity. Agron. J. 104:1336-47.
Nutini F, Confalonieri R, Paleari L, Pepe M, Criscuolo L, Porta F, Ranghetti L, Busetto L, Boschetti M, 2021. Supporting operational site-specific fertilization in rice cropping systems with infield smartphone measurements and Sentinel-2 observations. Precis. Agric. 1-20.
Österreichische Hagelversicherung, 2013. Österreichische Hagelversicherung, 27. Dezember 2013. In: Österreichische Hagelversicherung. Available from: https://www.hagel.at/
Peralta N, Assefa Y, Du J, Barden C, Ciampitti I, 2016. Mid-season high-resolution satellite imagery for forecasting site-specific corn yield. Remote Sens. 8:848.
Prabhakar M, Gopinath KA, Reddy AGK, Thirupathi M, Rao CS, 2019. Mapping hailstorm damaged crop area using multispectral satellite data. Egypt J. Remote Sens. Sp. Sci. 22:73-9.
Schillaci C, Tadiello T, Acutis M, Perego A, 2021. Reducing top-dressing N fertilization with variable rates does not reduce maize yield. Sustain 13:8059.
Shah A, Agarwal R, Baranidharan B, 2021. Crop yield prediction using remote sensing and meteorological data. Proc. Int. Conf. Artif. Intell. Smart Syst. ICAIS 2021:952-60.
Sibley AM, Grassini P, Thomas NE, Cassman KG, Lobell DB, 2014. Testing remote sensing approaches for assessing yield variability among maize fields. Agron. J. 106:24-32.
Sosa L, Justel A, Molina Í, 2021. Detection of crop hail damage with a machine learning algorithm using time series of remote sensing data. Agronomy 11:2078.
Szantoi Z, Geller GN, Tsendbazar NE, See L, Griffiths P, Fritz S, Gong P, Herold M, Mora B, Obregón A, 2020. Addressing the need for improved land cover map products for policy support. Environ. Sci. Policy 112:28-35.
Talukdar G, Sarma AK, Bhattacharjya RK, 2020. Mapping agricultural activities and their temporal variations in the riverine ecosystem of the Brahmaputra River using geospatial techniques. Remote Sens. Appl. Soc. Environ. 20:100423.
Toeglhofer C, Mestel R, Prettenthaler F, 2012. Weather value at risk: on the measurement of noncatastrophic weather risk. Weather Clim. Soc. 4:190-9.
Toreti A, Cronie O, Zampieri M, 2019. Concurrent climate

extremes in the key wheat producing regions of the world. Sci. Rep. 9:5493.
Verrelst J, Rivera JP, Moreno J, Camps-Valls G, 2013. Gaussian processes uncertainty estimates in experimental Sentinel-2 LAI and leaf chlorophyll content retrieval. ISPRS J. Photogramm. Remote Sens. 86:157-67.
Verrelst J, Rivera JP, Veroustraete F, Muñoz-Marí J, Clevers JGPW, Camps-Valls G, Moreno J, 2015. Experimental Sentinel-2 LAI estimation using parametric, non-parametric and physical retrieval methods - A comparison. ISPRS J. Photogramm. Remote Sens. 108:260-72.
Vescovo L, Gianelle D, Dalponte M, Miglietta F, Carotenuto F, Torresan C, 2016. Hail defoliation assessment in corn (Zea mays L.) using airborne LiDAR. F. Crop Res. 196:426-37.
Vroege W, Finger R, 2020. Insuring weather risks in european agriculture. EuroChoices 19:54-62.
Vuolo F, Neuwirth M, Immitzer M, Atzberger C, Ng WT, 2018. How much does multi-temporal Sentinel-2 data improve crop type classification? Int. J. Appl. Earth Obs. Geoinf. 72:122-30.
Vyas S, Dalhaus T, Kropff M, Aggarwal P, Meuwissen MPM, 2021. Mapping global research on agricultural insurance. Environ Res Lett. 16:103003.
Wang J, Ding J, Yu D, Ma X, Zhang Z, Ge X, Teng D, Li X, Liang J, Lizaga I, Chen X, Yuan L, Guo Y, 2019. Capability of Sentinel-2 MSI data for monitoring and mapping of soil salinity in dry and wet seasons in the Ebinur Lake region, Xinjiang, China. Geoderma 353:172-87.
Xiong J, Thenkabail PS, Gumma MK, Teluguntla P, Poehnelt J, Congalton RG, Yadav K, Thau D, 2017. Automated cropland mapping of continental Africa using Google Earth Engine cloud computing. ISPRS J Photogramm. Remote Sens. 126:225-44.